Available online at www.sciencedirect.com
SCIENCE DIRECT®
International Journal of Mass Spectrometry 227 (2003) 315–325
International Journal of Mass Spectrometry
www.elsevier.com/locate/ijms

Stationary points for the $OH^- + CH_3F \rightarrow CH_3OH + F^-$ potential energy surface

Lipeng Sun[a], Kihyung Song[a], William L. Hase[a,*], Marcelo Sena[b], Jose M. Riveros[b]

[a] *Department of Chemistry, Wayne State University, Detroit, MI 48202, USA*
[b] *Institute of Chemistry, University of São Paulo, Caixa Postal 26077, São Paulo CEP 05599-970, São Paulo, Brazil*

Received 3 January 2002; accepted 29 April 2002

Abstract

Ab initio calculations at the HF, MP2, and CCSD(T) levels of theory, utilizing a range of basis sets including the large bases 6-311++G(2df,2pd) and aug-cc-pVTZ, are used to study the $OH^- + CH_3F \rightarrow CH_3OH + F^-$ potential energy surface (PES). Structures, vibrational frequencies, and energies are determined for the reactant and product asymptotic limits, the $OH \cdots CH_3F$ ion–dipole potential minimum, the $[OH \cdots CH_3 \cdots F]^-$ central barrier, and the $CH_3OH \cdots F^-$ hydrogen-bonded minimum. This PES does not have a post-reaction $F^- \cdots CH_3OH$ minimum complementary to the pre-reaction $OH^- \cdots CH_3F$ minimum. Except for the $CH_3OH \cdots F^-$ minimum, the large basis sets and MP2 theory give a consistent set of structures and frequencies for the stationary points. Neither the structure nor the vibrational frequencies of the $CH_3OH \cdots F^-$ minimum are converged by the MP2 and large basis set calculations. RHF theory does not describe the energy of the $[OH \cdots CH_3 \cdots F]^-$ central barrier nor the reaction exothermicity, however, it does give $OH^- + CH_3F \rightarrow OH^- \cdots CH_3F$ and $F^- + CH_3OH \rightarrow CH_3OH \cdots F^-$ well depths in good agreement with the CCSD(T) values. Overall good agreement is found between the MP2/6-31+G* and much higher level CCSD(T) energies for the stationary points. The MP2 and CCSD(T) calculations give a reaction exothermicity and $F^- + CH_3OH \rightarrow CH_3OH \cdots F^-$ well depth in good agreement with the experimental values.

Keywords: Potential energy surface; S_N2 reactions; Ion–dipole potential

1. Introduction

Bimolecular nucleophilic substitution (S_N2) reactions of the type.

$$X^- + CH_3Y \rightarrow XCH_3 + Y^- \quad (1)$$

have been studied as prototype reactions in gas-phase ion–molecule chemistry for the past two decades [1–4]. Extensive investigations, both theoretical [5–17] and experimental [18–27], have been carried out to understand the energies and dynamics of reaction (1). The study of these simple bimolecular reactions has provided fundamental information concerning the intrinsic mechanisms for S_N2 reactions. Also, the theoretical predictions, when compared with experimental results, serve as tests of statistical models for chemical reaction rates [12,24,28,29].

The most commonly studied systems in reaction (1) are reactions of halide ions with methyl halides; e.g., $Cl^- + CH_3Br$. The potential energy surface (PES) for this class of reactions is characterized by

* Corresponding author. Tel.: +1-313-577-2694; fax: +1-313-577-8822.
E-mail address: wlh@chem.wayne.edu (W.L. Hase).

1387-3806/03/$ – see front matter © 2003 Elsevier Science B.V. All rights reserved.
doi:10.1016/S1387-3806(03)00096-4

a double-well model [30,31], in which the wells corresponding to $X^- \cdots CH_3Y$ and $XCH_3 \cdots Y^-$ are separated by the $[X \cdots CH_3 \cdots Y]^-$ central barrier. From experiments [32] and classical trajectory [2,33] and quantum dynamical simulations [34,35], extensive non-statistical dynamics has been observed for these reactions. Included amongst the non-statistical dynamics is a direct reaction pathway without trapping in either the $X^- \cdots CH_3Y$ or $XCH_3 \cdots Y^-$ potential energy well [36], mode specific decomposition of the $X^- \cdots CH_3Y$ and $XCH_3 \cdots Y^-$ complexes with inefficient intramolecular vibrational energy distribution [2,34,36,37], extensive recrossings of the $[X \cdots CH_3 \cdots Y]^-$ central barrier region of the PES [38], non-statistical energy distributions of the reaction products [23], and a dependence of the reaction rate on translational, rotational and vibrational energies inconsistent with the statistical model [2,24,28,29]. In contrast to the richness of these non-statistical dynamics, the statistical model gives a rate constant for $Cl^- + CH_2CN \rightarrow ClCH_2CN + Cl^-$ in excellent agreement with the experimental value [39].

As discussed above, for most of the studied S_N2 reactions, the nucelophiles are halide ions, which are weak bases. An immediate question is whether the reaction mechanism is altered if one uses a stronger base such as OH^- for the nucleophile. Early experimental studies of the S_N2 kinetics of OH^-, utilizing the flowing afterflow technique, were carried out by Bohme and co-workers [40] and Bierbaum and co-workers [20]. They systematically measured the rates of a series of reactions including

$$OH^- + CH_3F \rightarrow CH_3OH + F^- \quad (2)$$

which proceeds with a much slower rate than the similar reaction with other methyl halides. Though these studies provide valuable information about the S_N2 kinetics of the OH^- nucleophile, they do not identify the S_N2 reaction mechanisms or details of the PESs. Preliminary information about the latter has been determined from ab initio calculations. Ab initio molecular orbital calculations for OH^- reacting with CH_3Cl [41] show a double-well PES. However, instead of forming a traditional back-side $HOCH_3 \cdots Cl^-$ ion–dipole potential minimum in the exit-channel, a minimum was found in which Cl^- is bound to CH_3OH via a hydrogen bond, i.e., $CH_3OH \cdots Cl^-$. With electron correlation included in the calculations, a value of 54 kcal/mol was determined for the $OH^- + CH_3Cl \rightarrow CH_3OH + Cl^-$ heat of reaction, which is in very good agreement with the value of -50 ± 5 kcal/mol determined from the Lias et al. [42] compilation of heats of formation. The hydrogen bond of $CH_3OH \cdots Cl^-$ gives a well depth of 15.5 kcal/mol with respect to the products.

Stationary points for reaction (2) have also been studied by ab initio methods [43–46]. Early ab initio calculations of stationary points of the PES by Černušák and co-workers [43] gave a reaction enthalpy in qualitative agreement with experiment. The uncertainty of the experimental reaction exothermicity comes in part from the uncertainty of the CH_3F standard enthalpy of formation which is known to only ±2 kcal/mol [47]. These early studies illustrated the importance of including electron correlation in determining accurate properties of the PES for reaction (2). Recently, stationary points for reaction (2) have been studied at the MP2/6-311++G(3dp,3df) level of theory [45] and the accuracy of DFT for describing the energies of the stationary points has been investigated [46]. These calculations show there is a traditional pre-reaction backside S_N2 ion–dipole potential energy well, i.e., $OH^- \cdots CH_3F$, and that the energy of the $[OH \cdots CH_3 \cdots F]^-$ central barrier is only slightly lower than that of the reactants. The exit-channel does not have a traditional backside S_N2 potential energy well (i.e., $F^- \cdots CH_3OH$) and only a minimum for the $CH_3OH \cdots F^-$ hydrogen-bonded structure is found. A particularly interesting attribute of reaction (2) is its slow rate, even though it is highly exothermic [45].

In the work presented here, these previous ab initio studies are extended to determine structures, vibrational frequencies and energies for reaction (2). These calculations provide insight into the level of electronic structure theory required to obtain a quantitative PES for reaction (2). Of particular interest is the identification of the level of theory which will give a reliable potential energy surface which may be used in direct dynamics simulations [48].

2. Electronic structure methods

The ab initio electronic structure calculations reported here were performed with the Gaussian 98 computer program [49]. The self-consistent field (SCF), second-order Møller–Plesset perturbation (MP2), coupled-cluster singles-and-doubles (CCSD) [50], and CCSD with perturbative triples correction [CCSD(T)] [51,52] theoretical methods were used. The basis sets used in the calculations range from the 6-31G* split valence basis set to the much larger 6-311++G(2df,2pd) and aug-cc-pVTZ bases. The stationary points were determined for the $OH^- + CH_3F$ reactants, $HO^- \cdots CH_3F$ potential energy minimum, $[HO \cdots CH_3 \cdots F]^-$ central barrier, $CH_3OH \cdots F^-$ potential energy minimum and $CH_3OH + F^-$ products. These are the only stationary points on the PES, and geometries, harmonic vibrational frequencies and energies were calculated for them. The effect of basis set superposition error (BSSE) on the $OH^- + CH_3F$ and $F^- + CH_3OH$ complexation energies was not included. Previous work [46] has shown that the BSSE, obtained by the counterpoise procedure [53,54], is generally less than 0.5 kcal/mol for S_N2 reactions similar to the one studied here and calculations with the aug-cc-pVTZ basis set.

3. Results

3.1. Geometries

The geometries of the stationary points, optimized at the RHF and MP2 levels of theory, with different basis sets, are listed in Table 1 . The MP2/6-31+G* and MP2/6-311++G(2df,2pd) geometries for the $OH^- \cdots CH_3F$ and $CH_3OH \cdots F^-$ potential energy minima and $[HO \cdots CH_3 \cdots F]^-$ barrier are depicted in Fig. 1. Overall, the MP2 geometries calculated with the 6-31+G* and larger basis sets are in very good agreement. The exception to this finding is the $CH_3OH \cdots F^-$ minimum, where using the 6-31+G* basis instead of the largest basis, results in a H–F bond that is 0.14 Å longer and a O–H bond that is 0.03 Å shorter. Also given in Table 1 are the CCSD(T)/TZ2Pf+dif geometries determined by Gonzales et al. [46]. Overall, the MP2 geometries with the large basis sets are in good agreement with these CCSD(T) geometries.

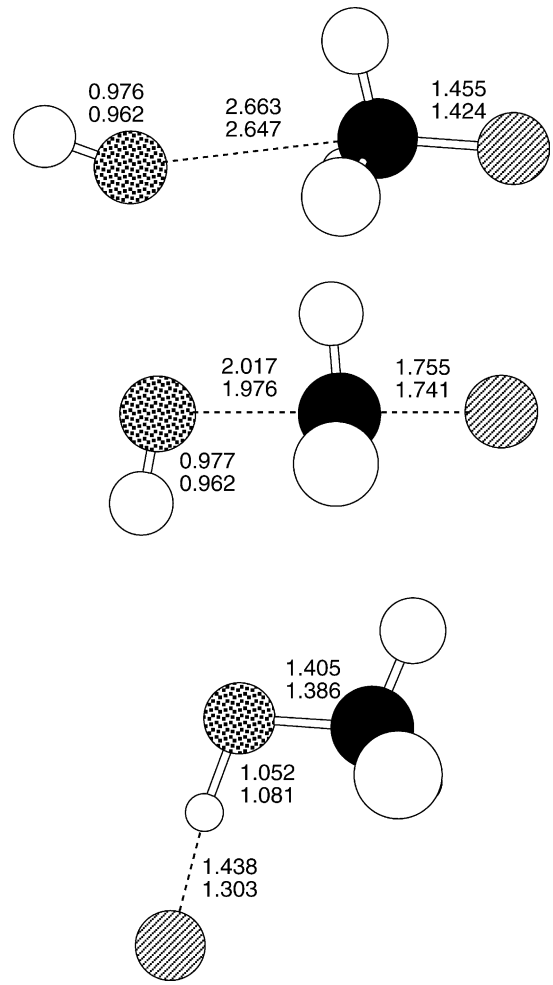

Fig. 1. MP2/6-31+G* and 6-311++G(2df,2pd) geometries for the $HO^- \cdots CH_3F$ well, $[HO \cdots CH_3 \cdots F]^-$ barrier, and $CH_3OH \cdots F^-$ well. The lower set of bond distances, in Å, are for the 6-31+G* basis set.

As found for other S_N2 ion–dipole minima, there is little change in the structure of the molecule as the anion binds. For the $HO^- \cdots CH_3F$ minimum the C–F bond length increases by 0.04–0.05 Å, while the C–O bond length decreases by 0.03 Å upon forming

Table 1
Geometries of the $OH^- + CH_3F \rightarrow F^- + CH_3OH$ stationary points[a]

Theory	Geometry[b]				
	$OH^- + CH_3F$				
	R(C–F)	R(C–H)	R(O–H)	F–C–H	H–C–H
RHF/6-31G*	1.365	1.082	0.962	109.1	109.9
RHF/6-31+G*	1.372	1.081	0.953	108.5	110.4
RHF/6-31++G**	1.372	1.082	0.948	108.5	110.4
RHF/6-311++G**	1.366	1.082	0.945	108.8	110.2
MP2/6-31G*	1.392	1.092	0.981	109.1	109.8
MP2/6-31+G*	1.407	1.091	0.977	108.0	110.9
MP2/6-31++G*	1.405	1.087	0.971	108.2	110.7
MP2/6-311++G**	1.389	1.091	0.971	108.7	110.2
MP2[c]	1.383	1.086	0.963	108.9	110.0
CCSD(T)[d]	1.388	1.086	0.965	108.8	110.1
Expt.[e]	1.382	1.090		108.4	110.5
	$HO^- \cdots CH_3F$				
	R(C–F)	R(C–O)	F–C–O	H–O–C	F–C–H
RHF/6-31G*	1.407	2.698	174.6	102.3	108.7(108.6)
RHF/6-31+G*	1.415	2.727	178.4	176.6	108.4(108.2)
RHF/6-31++G**	1.415	2.726	175.6	170.5	108.8(108.4)
RHF/6-311++G**	1.408	2.739	175.6	167.0	108.3(108.9)
MP2/6-31G*	1.427	2.861	124.5	95.0	113.9(106.9)
MP2/6-31+G*	1.455	2.663	169.0	153.3	107.0(108.3)
MP2/6-31++G**	1.451	2.657	168.6	152.0	107.1(108.5)
MP2/6-311++G**	1.432	2.680	168.1	149.5	108.2(109.3)
MP2[c]	1.424	2.647	168.6	155.8	108.2(109.6)
CCSD(T)[d]	1.429	2.656	168.8	157.5	108.1(109.4)
	$[HO \cdots CH_3 \cdots F]^-$				
	R(C–F)	R(C–O)	F–C–O	H–O–C	F–C–H
RHF/6-31G*	1.768	1.930	178.8	105.7	92.2(91.1)
RHF/6-31+G*	1.791	1.992	177.6	112.3	92.8(91.6)
RHF/6-31++G**	1.790	1.990	177.3	114.9	92.9(91.7)
RHF/6-311++G**	1.798	1.995	177.5	113.1	92.7(91.6)
MP2/6-31G*	1.732	1.944	179.0	100.4	93.9(92.5)
MP2/6-31+G*	1.755	2.017	177.1	108.8	94.4(93.0)
MP2/6-31++G**	1.758	2.004	177.3	108.2	94.1(92.7)
MP2/6-311++G**	1.755	1.987	177.4	106.3	93.8(92.6)
MP2[c]	1.741	1.976	177.9	104.0	93.8(92.8)
CCSD(T)[d]	1.753	2.000	177.9	104.2	94.0(93.0)
	$CH_3OH \cdots F^-$				
	R(H–F)	R(O–H)	R(C–O)	F–H–O	H–O–C
RHF/6-31G*	1.252	1.090	1.364	172.9	105.4
RHF/6-31+G*	1.492	1.003	1.378	173.2	108.1
RHF/6-31++G**	1.461	1.004	1.376	173.8	108.4
RHF/6-311++G**	1.472	0.999	1.375	173.3	107.9
MP2/6-31G*	1.139	1.227	1.377	173.2	103.3
MP2/6-31+G*	1.438	1.052	1.405	174.0	106.3
MP2/6-31++G**	1.373	1.061	1.400	175.3	106.4

Table 1 (*Continued*)

Theory	Geometry[b]				
MP2/6-311++G**	1.340	1.063	1.391	176.6	105.4
MP2[c]	1.303	1.081	1.386	176.6	106.2
CCSD(T)[d]	1.336	1.064	1.392	176.1	105.9
	$CH_3OH + F^-$				
	R(C–O)	R(C–H)	R(O–H)	H–O–C	H–C–O
RHF/6-31G*	1.399	1.081(1.087)	0.946	109.5	107.2(112.0)
RHF/6-31+G*	1.402	1.080(1.087)	0.946	110.4	107.0(111.7)
RHF/6-31++G**	1.401	1.081(1.087)	0.942	110.5	107.1(111.8)
RHF/6-311++G**	1.400	1.082(1.087)	0.940	110.0	107.3(111.8)
MP2/6-31G*	1.425	1.090(1.097)	0.970	107.3	106.3(112.3)
MP2/6-31+G*	1.431	1.089(1.096)	0.972	108.7	105.9(111.7)
MP2/6-31++G**	1.429	1.086(1.092)	0.964	108.5	106.2(111.8)
MP2/6-311++G**	1.422	1.090(1.096)	0.959	107.3	106.7(112.0)
MP2	1.420	1.085(1.090)	0.958	108.1	106.7(112.1)
CCSD(T)[d]	1.424	1.085(1.090)	0.959	107.9	106.8(111.9)
Expt.[e]	1.421	1.094[f]	0.963	108.0	107.2(112.0)

[a] Bond lengths are in angstroms (Å) and angles are in degrees (°).
[b] Data in parentheses are for the degenerate internal coordinates.
[c] Basis set used in the geometry optimization is 6-311++G(2df,2pd).
[d] The basis set is TZ2Pf+dif and the calculations are from ref. [46].
[e] Refs. [58,63], respectively.
[f] Methyl group is assumed to be symmetric.

the $CH_3OH \cdots F^-$ minimum. These different effects on the molecular bond length, i.e., increasing and decreasing, results from a standard back-side S_N2 structure for $HO^- \cdots CH_3F$ and a hydrogen bond structure for $CH_3OH \cdots F^-$. The geometry of the $F^- \cdots CH_3F$ minimum has been studied previously [55], and the geometric change of CH_3F in $HO^- \cdots CH_3F$ is larger than that in $F^- \cdots CH_3F$ because OH^- is a stronger base than F^-. The loss of C_{3v} symmetry for $HO^- \cdots CH_3F$ arises from the anisotropic field OH^- introduces on CH_3F. Though the C–F and C–O bonds of the reactant and product molecules CH_3F and CH_3OH are similar in length (i.e., they differ by only 0.02–0.04 Å at the MP2 level) the C–O bond at the central barrier is 0.22–0.26 Å larger than the C–F bond. This result is consistent with an early transition state, i.e., central barrier, for the exothermic $OH^- + CH_3F \rightarrow CH_3OH + F^-$ reaction.

The O–H bond length has small changes during the course of the reaction. Starting from the $OH^- + CH_3F$ stationary point, the O–H bond length for the five stationary points are 0.977, 0.976, 0.977, 1.052, and 0.972 Å at the MP2/6-31+G* level and 0.963, 0.962, 0.962, 1.081, and 0.958 Å at the MP2/6-311++G(2df,2pd) level. There are similar small changes in the C–H bond length. For these respective five stationary points, the C–H bond length is 1.091, 1.088(1.084), 1.075, 1.099(1.103), and 1.089(1.096) Å at the MP2/6-31+G* level and 1.086, 1.082(1.080), 1.070, 1.097(1.101), and 1.085(1.090) Å at the MP2/6-311++G(2df,2pd) level (the numbers in parentheses are for the two C–H bonds with identical lengths). As found for other S_N2 reactions, the C–H bond shortens as the reactive system approaches the central barrier from either the reactants or products [6,13,14,56].

3.2. Vibrational frequencies

In previous work, ab initio calculations have been used to determine vibrational frequencies for OH^-, CH_3F, CH_3OH, the $HO^- \cdots CH_3F$

and $CH_3OH\cdots F^-$ minima [13,43,57], and the $[HO\cdots CH_3\cdots F]^-$ central barrier [43]. A larger basis set is used for the frequency calculations reported here. Harmonic vibrational frequencies for the stationary points, calculated at the MP2 level of theory with the 6-31+G* and 6-311++G(2df,2pd) basis sets, are summarized in Table 2. The agreement between the calculated and experimental harmonic frequencies for CH_3F is quite good, particularly for the larger basis set calculation. As expected, the experimental anharmonic OH and CH stretching frequencies for CH_3OH are considerably lower than the ab initio values.

The change in vibrational frequencies, as the reactive system moves from the reactant to product stationary points, is similar to what has been found for other S_N2 reactions [6,13,56]. There are only relatively small changes in the frequencies for the CH_3 rock, CH_3 deformation, and CH_3 stretch modes. The slight increase in the CH_3 stretch frequencies, in moving from either the reactants or products to the central barrier, is consistent with the shortening of the C–H bonds. Both this increase in the C–H stretch frequencies and shortening of the C–H bonds is a normal property of S_N2 reactions defined by reaction (1).

The vibrational frequencies for the $OH^-\cdots CH_3F$ back-side potential energy minimum and $[HO\cdots CH_3\cdots F]^-$ central barrier are consistent with frequencies of these stationary points for the $Cl^- + CH_3Cl$, $Cl^- + CH_3Br$, and $F^- + CH_3Cl$ potential energy surfaces [7,13,56]. As noted previously by Brauman and co-workers [57] there are several interesting properties amongst the frequencies of the $CH_3OH\cdots F^-$ hydrogen-bonded potential energy minimum. There is a substantial lowering of the OH stretch frequency when F^- forms the strong hydrogen bond with CH_3OH. In addition, the two frequencies associated with $O–H\cdots F^-$ bend are strikingly different. This difference is a result of both mass and force constant effects. For the mode with lower frequency, the reduced mass is 3.47 amu and the force constant is 0.0534 mdyn/Å. These values are 1.04 amu and 0.8280 mdyn/Å for the higher frequency mode.

There is nearly a two-orders-of-magnitude difference in the intensities for the OH stretch mode in methanol and in the $CH_3OH\cdots F^-$ complex. Their intensities are 34.76 and 2389, respectively, at the MP2/6-31+G* level of theory. The complex resembles a proton-bound dimer of methoxide and fluoride and its increased charge separation dramatically increases the intensity of the OH strectch.

3.3. Energies

Energies for the stationary points on the PES, calculated at the different levels of electronic structure theory and with different basis sets, are listed in Table 3. Also given in Table 3 are the CCSD(T)/TZ2Pf+dif energies presented previously by Gonzales et al. [46]. Overall, these CCSD(T) energies and the CCSD(T)/aug-cc-pVTZ values reported here are in very good agreement. The energies calculated with the MP2/6-31+G* and CCSD(T)/aug-cc-pVTZ methods are depicted in Fig. 2. The results in Table 3 show that the inclusion of diffuse functions in the basis is necessary to obtain accurate energies and Hartree–Fock (HF) theory gives an inaccurate energy for the $[HO\cdots CH_3\cdots F]^-$ central barrier and an inaccurate heat of reaction. The latter is consistent with previous calculations for $OH^- + CH_3Y$ (Y = F, Cl) [41,43–46], which show that treating electron correlation is needed to have an accurate potential energy profile. However, the HF calculations do give accurate well depths. For the 6-31+G* and larger basis sets, the HF well depth for $OH^-\cdots CH_3F$ complex is 13–14 kcal/mol while the MP2 and CCSD(T) values range from 14 to 15 kcal/mol. Using the same basis, the HF well depth for the $CH_3OH\cdots F^-$ complex, with respect to the $CH_3OH + F^-$ products is 26 kcal/mol while the MP2 and CCSD(T) well depths are 29–33 kcal/mol. These well depths are in good agreement with the experimental result of $\Delta H^\circ_{298} =$ 29.6 kcal/mol [61,62]. The calculated values for the $OH^- + CH_3F \rightarrow CH_3OH + F^-$ reaction exothermicity are in good agreement with the experimental value of 18 ± 9 kcal/mol [40].

Fig. 2 shows that MP2 theory with the 6-31+G* basis gives energies for the stationary points in overall good agreement with those for the much

Table 2
Harmonic frequencies for $OH^- + CH_3F \rightarrow F^- + CH_3OH$ stationary points[a]

Mode	MP2/6-31+G*	MP2/6-311++G(2df,2pd)	Expt.[b]
	$OH^- + CH_3F$		
CF stretch	1052	1086	1078
CH_3 rock	1212(2)[c]	1211(2)	1204(2), 1496, 1515(2)
CH_3 deformation	1525, 1551(2)	1505, 1521(2)	3075, 3147(2)
CH_3 stretch	3125, 3236(2)	3097, 3199(2)	
OH stretch	3702	3844	
	$OH^- \cdots CH_3F$		
OH torsion	58	72	
CH_3F rock	116, 177	107, 188	
OC stretch	188	193	
OH^- bend	227	212	
CF stretch	902	954	
CH_3 rock	1125, 1153	1127, 1157	
CH_3 deformation	1429, 1521, 1527	1416, 1497, 1501	
CH_3 stretch	3186, 3310, 3327	3150, 3263, 3278	
OH stretch	3725	3857	
	$[HO \cdots CH_3 \cdots F]^-$		
OCF asymmetric stretch	582i	606i	
OH torsion	149	145	
OCF bend	304, 327	314, 336	
OCF symmetric stretch	366	375	
OH^- bend	674	699	
CH_3 rock	1125, 1142	1100, 1128	
CH_3 deformation	1260, 1443(2)	1228, 1414(2)	
CH_3 stretch	3222, 3422, 3426	3189, 3389, 3390	
OH stretch	3716	3861	
	$CH_3OH \cdots F^-$		
CH_3 torsion	87	65	
F^- bend	162	170	
OHF^- bend	1163	1162	
F^- stretch	361	447	
CO stretch	1123	1141	
CH_3 rock	1176, 1199	1181, 1287	
CH_3 deformation	1502, 1536, 1561	1451, 1493, 1519	
COH bend	1625	1655	
OH stretch	2392	1875	
CH_3 stretch	3009, 3029, 3093	2960, 2988, 3031	
	CH_3OH		
CH_3 torsion	332	293	295
CO stretch	1065	1063	1033
CH_3 rock	1090, 1197	1097, 1186,	1060, 1165
COH bend	1385	1377	1345
CH_3 deformation	1524, 1552, 1562	1493, 1520, 1532	1455, 1477, 1477
CH_3 stretch	3083, 3155, 3227	3064, 3136, 3196	2844, 2960, 3000
OH stretch	3776	3908	3681

[a] Frequencies are in units of cm^{-1}.
[b] The experimental frequencies of CH_3F and CH_3OH are from refs. [59,60], respectively. Those for CH_3F are harmonic frequencies and those for CH_3OH are anharmonic $1 \leftarrow 0$ fundamental frequencies.
[c] The data in parentheses indicate a two-fold degeneracy of normal mode frequencies.

Table 3
Energies of the $OH^- + CH_3F \rightarrow F^-CH_3OH$ stationary points[a]

Theory	Stationary points			
	$HO^- \cdots CH_3F$	$[HO \cdots CH_3 \cdots F]^-$	$CH_3OH \cdots F^-$	$F^- + CH_3OH$
RHF/6-31G*	−18.07	−1.79	−58.48	−15.49
RHF/6-31+G*	−13.37	3.36	−50.31	−24.41
RHF/6-31++G**	−13.56	3.72	−49.54	−23.68
RHF/6-311++G**	−13.22	5.09	−48.94	−23.35
MP2/6-31G*	−23.55	−12.30	−68.19	−14.90
MP2/6-31+G*	−14.89	−5.05	−53.55	−24.99
MP2/6-31++G**	−15.10	−4.62	−52.80	−23.67
MP2/6-311++G**	−14.21	−1.32	−52.50	−22.78
MP2[b]	−14.10	−2.99	−52.21	−19.94
CCSD(T)[c]	−14.36	−3.91	−52.43	−19.84
CCSD(T)[d]	−13.91	−3.02	−49.95	−19.59
CCSD(T)[e]	−13.78	−3.05	−50.88	−20.80
Expt.	–	–	–[f]	−18 ± 9[g]

[a] Energies, with respect to the reactants, are in kcal/mol. Zero-point energies are not included.
[b] Basis set used is 6-311++G(2df,2pd).
[c] CCSD(T)/6-311++G(2df,2pd)//MP2/6-311++G(2df,2pd) calculation.
[d] CCSD(T)/aug-cc-pVTZ//MP2/6-311++G(2df,2pd) calculation.
[e] Basis set is TZ2Pf+dif and the calculations are from ref. [46].
[f] The MP2 and CCSD(T) values for the $F^- + CH_3OH \rightarrow CH_3OH \cdots F^-$ well depth are in excellent agreement with the experimental value of $\Delta H^\circ_{298} = 29.6$ kcal/mol [61,62].
[g] The experimental result is from ref. [40].

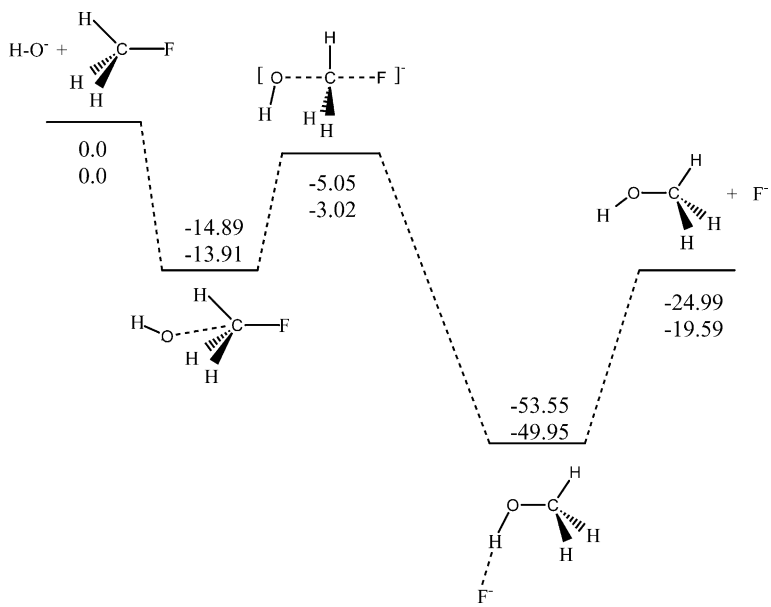

Fig. 2. MP2/6-31+G* and CCSD(T)/aug-cc-pVTZ//MP2/6-311++G(2df,2pd) energies for the stationary points along the intrinsic reaction coordinate. The lower set of energies, in kcal/mol, are for the 6-31+G* basis set.

higher level CCSD(T)/aug-cc-pVTZ calculation based on the MP2/6-311++G(2df,2pd) geometries. The $CH_3OH\cdots F^-$ well depth is 29 and 30 kcal/mol for the MP2/6-31+G* and higher level CCSD(T) calculation, respectively. Though the agreement in the energy difference between the $[HO\cdots CH_3\cdots F]^-$ central barrier and $F^- + CH_3OH$ products is not as good, it is still quite satisfactory. The MP2/6-31+G* value is 20 kcal/mol while CCSD(T) gives 17 kcal/mol. The overall good agreement, between the MP2/6-31+G* energies and those of the much higher level of CCSD(T) calculations, demonstrates that this MP2 model gives an accurate PES. This is a very important finding, since MP2/6-31+G* is a tractable and practical model for direct dynamics simulations of the $OH^- + CH_3F$ reaction dynamics [48].

4. Summary

In the work presented here ab initio calculations at the RHF, MP2, and CCSD(T) levels of theory, with a range of basis sets, are used to explore the $OH^- + CH_3F \rightarrow CH_3OH + F^-$ potential energy surface. Structures, vibrational frequencies, and energies are calculated for the five stationary points on the PES; i.e., the reactant and product asymptotic limits, the $OH^-\cdots CH_3F$ ion–dipole potential minimum, the $[OH\cdots CH_3\cdots F]^-$ central barrier, and the $CH_3OH\cdots F^-$ hydrogen-bonded potential minimum. The following summarizes the results presented here.

1. The qualitative change in the structures of the stationary points, as the reactive system moves from reactants to products, is the same as found for other S_N2 reactions. Except for the $CH_3OH\cdots F^-$ potential minimum, the large 6-311++G** and 6-311++G(2df,2pd) basis sets and MP2 theory give nearly identical geometries for each stationary point. These two basis sets give $H\cdots F^-$ and O–H bond lengths for $CH_3OH\cdots F^-$ which differ by 0.04 and 0.02 Å, respectively.
2. There is an ∼0.25 Å extension of the C–O bond at the central barrier, which is consistent with an early transition state for an exothermic reaction.
3. MP2/6-31+G* and MP2/6-311++G(2df,2pd) frequencies are in good agreement for each stationary point on the PES except for $CH_3OH\cdots F^-$. The overall lack of agreement in the $CH_3OH\cdots F^-$ frequencies, for these two calculations, is consistent with the two calculations' significantly different $H\cdots F^-$, C–O, and O–H bond lengths.
4. RHF theory, with the 6-31+G* and larger basis, gives $OH^- + CH_3F \rightarrow OH^-\cdots CH_3F$ and $F^- + CH_3OH \rightarrow CH_3OH\cdots F^-$ well depths which are in good agreement with the CCSD(T) values. However, RHF theory gives an inaccurate $[OH\cdots CH_3\cdots F]^-$ central barrier energy and reaction exothermicity, and electron correlation is required in the calculations to determine the accurate values for these energies.
5. Overall good agreement is found between the MP2/6-31+G* and much higher level of CCSD(T) energies for the stationary points. The $OH^- + CH_3F \rightarrow F^- + CH_3OH$ reaction exothermicity calculated at the MP2 and CCSD(T) levels and the $F^- + CH_3OH \rightarrow CH_3OH\cdots F^-$ well depth calculated at the RHF, MP2 and CCSD(T) levels, with the 6-31+G* and larger basis sets, are in good agreement with the experimental values [40,61,62].

Acknowledgements

This research was supported by the National Science Foundation, by the São Paulo Science Foundation (FAPESP) and by the American Chemical Society though its International Activities program.

References

[1] C.R. Moylan, J.I. Brauman, in: W.L. Hase (Ed.), Advances in Classical Trajectory Methods, vol. 2, JAI Press, New York, 1994, p. 95.
[2] W.L. Hase, Science 266 (1994) 988.
[3] S.L. Craig, J.I. Brauman, Science 276 (1997) 1536.
[4] S.S. Shaik, H.B. Schlegel, S. Wolf, Theoretical Aspects of Physical Organic Chemistry. The S_N2 Mechanism. Wiley, New York, 1992.

[5] V.M. Ryaboy, in: W.L. Hase (Ed.), Advances in Classical Trajectory Methods, vol. 12, JAI Press, New York, 1994, p. 115.
[6] S.R. Vande Linde, W.L. Hase, J. Am. Chem. Soc. 111 (1989) 2349;
S.R. Vande Linde, W.L. Hase, J. Phys. Chem. 94 (1990) 6148;
S.R. Vande Linde, W.L. Hase, J. Phys. Chem. 94 (1990) 2778;
S.R. Vande Linde, W.L. Hase, J. Chem. Phys. 102 (1990) 5626.
[7] S.C. Tucker, D.G. Truhlar, J. Am. Chem. Soc. 112 (1990) 3338;
S.C. Tucker, D.G. Truhlar, J. Phys. Chem. 93 (1989) 8138.
[8] Y.J. Cho, S.R. Vande Linde, L. Zhu, W.L. Hase, J. Chem. Phys. 96 (1992) 8275.
[9] G.D. Billing, Chem. Phys. 159 (1992) 109.
[10] H. Wang, W.L. Hase, Chem. Phys. 212 (1996) 247.
[11] O.V. Gritsenko, B. Ensing, P.R.T. Schipper, E.J. Baerends, J. Phys. Chem. A 104 (2000) 8558.
[12] H. Wang, W.L. Hase, J. Am. Chem. Soc. 117 (1995) 9347.
[13] H. Wang, W.L. Hase, J. Am. Chem. Soc. 119 (1997) 3093.
[14] T. Su, H. Wang, W.L. Hase, J. Phys. Chem. A 102 (1998) 9819.
[15] H. Tachikawa, M. Igarashi, Chem. Phys. Lett. 303 (1999) 81.
[16] P. Botschwina, M. Horn, S. Seeger, R. Oswald, Ber. Bunsenges. Phys. Chem. 101 (1997) 387.
[17] M. Igarashi, H. Tachikawa, Int. J. Mass Spectrom. Ion Process 181 (1998) 151.
[18] W.E. Farneth, J.I. Brauman, J. Am. Chem. Soc. 98 (1976) 7891.
[19] M.J. Pellerite, J.I. Brauman, J. Am. Chem. Soc. 105 (1983) 2672.
[20] C.H. DePuy, S. Gronert, A. Mullin, V.M. Bierbaum, J. Am. Chem. Soc. 112 (1990) 8650.
[21] D.M. Cyr, L.A. Posey, G.A. Bishea, C.-C. Han, A. Johnson, J. Am. Chem. Soc. 113 (1991) 9697.
[22] W.B. Knighton, J.A. Bognan, P.M. O'Connor, E.P. Grimsrud, J. Am. Chem. Soc. 115 (1993) 12079.
[23] S.T. Graul, M.T. Bowers, J. Am. Chem. Soc. 116 (1994) 3875.
[24] S.L. Graig, J.I. Brauman, J. Phys. Chem. A 101 (1997) 4745.
[25] C. Li, P. Ross, J.E. Szulejko, T.B. McMahon, J. Am. Chem. Soc. 118 (1996) 9360.
[26] J.-L. Le Garrec, B.R. Rowe, J.L. Queffelec, J.B.A. Mitchell, D.C. Clary, J. Chem. Phys. 107 (1997) 1021.
[27] L.A. Angel, K.M. Ervin, J. Phys. Chem. A 105 (2001) 4042.
[28] V.F. DeTuri, P.A. Hintz, K.M. Ervin, J. Phys. Chem. A 101 (1997) 5969.
[29] A.A. Viggiano, R.A. Morris, J.S. Paschkewitz, J.F. Paulson, J. Am. Chem. Soc. 114 (1992) 10477.
[30] W.N. Olmstead, J.I. Brauman, J. Am. Chem. Soc. 99 (1977) 4219.
[31] J.A. Dodd, J.I. Brauman, J. Phys. Chem. 90 (1986) 3559.
[32] M.L. Chabinyc, S.L. Craig, C.K. Regan, J.I. Brauman, Science 279 (1998) 1882.
[33] W.L. Hase, Acc. Chem. Res. 31 (1998) 659.
[34] S. Schmatz, P. Botschwina, J. Hauschildt, R. Schinke, J. Chem. Phys. 114 (2001) 5233.
[35] M.I. Hernandez, J. Campos-Martinez, P. Villarreal, S. Schmatz, D.C. Clary, Phys. Chem. Chem. Phys. 1 (1999) 1197.
[36] S.R. Vande Linde, W.L. Hase, J. Chem. Phys. 93 (1990) 7962.
[37] D.S. Tonner, T.B. McMahon, J. Am. Chem. Soc. 122 (2000) 8783.
[38] L. Sun, K. Song, W.L. Hase, J. Am. Chem. Soc. 123 (2001) 5753.
[39] A.A. Viggiano, R.A. Morris, T. Su, B.D. Wladkowski, S.L. Craig, M.L. Zhong, J.I. Brauman, J. Am. Chem. Soc. 116 (1994) 2213.
[40] K. Tanaka, G.I. Mackay, J.D. Payzant, D.K. Bohme, Can. J. Chem. 54 (1976) 1643.
[41] J. Evanseck, J.F. Blake, W.L. Jorgensen, J. Am. Chem. Soc. 109 (1987) 2349.
[42] S.G. Lias, J.E. Bartmess, J.F. Liebman, J.L. Holmes, R.D. Levin, W.G. Mallard, J. Phys. Chem. Ref. Data 17 (Suppl. 1) (1988) 1.
[43] M. Urban, I. Ĉernušák, V. Kellö, Chem. Phys. Lett. 105 (1984) 625;
I. Ĉernušák, G.H.F. Diercksen, Chem. Phys. Lett. 128 (1986) 538.
[44] Z. Shi, R.J. Boyd, J. Am. Chem. Soc. 112 (1990) 6789;
Z. Shi, R.J. Boyd, J. Am. Chem. Soc. 111 (1989) 1575.
[45] J.M. Riveros, M. Sena, G.H. Guedes, L.A. Xavier, R. Slepetys, Pure Appl. Chem. 70 (1998) 1969.
[46] J.M. Gonzales, R.S. Cox, S.T. Brown, W.D. Allen, H.F. Schaefer III, J. Phy. Chem. A 105 (2001) 11327.
[47] P.M. Hierl, M.J. Henchman, J.F. Paulson, Int. J. Mass Spectrom. Ion Process 117 (1992) 475.
[48] L. Sun, K. Song, W.L. Hase, Science 296 (2002) 875.
[49] M.J. Frish, G.W. Trucks, H.B. Schlegel, G.E. Scuseria, M.A. Robb, J.R. Cheeseman, V.G. Zakrzewski, J.A. Montgomery, Jr., R.E. Stratman, J.C. Burant, S. Dapprich, J.M. Milliam, A.D. Daniels, K.N. Kudin, M.C. Strain, O. Farkas, J. Tomasi, V. Barone, M. Cossi, R. Cammi, B. Mennucci, C. Pomelli, C. Adamo, S. Clifford, J. Ochterski, G.A. Petersson, P.Y. Ayala, Q. Cui, K. Morokuma, D.K. Malick, A.D. Rabuck, K. Raghavachari, J.B. Foresman, J. Cioslowski, J.V. Oritz, B.B. Stefanov, G. Liu, A. Liashenko, P. Piskorz, I. Komoaromi, R. Gomperts, R.L. Martin, D.J. Fox, T. Keither, M.A. Al-Laham, C.Y. Peng, A. Nanayakkara, C. Gonzalez, M. Challacoombe, P.M.W. Gille, B. Johnson, W. Chen, M.W. Wong, J.L. Andres, C. Gonzalez, M. Head-Gordon, E.S. Replogle, J.A. Pople, Gaussian 98, Gaussian, Inc., Pittsburgh, PA, 1998.
[50] G.D. Purvis III, R.J. Bartlett, J. Chem. Phys. 76 (1982) 1910.
[51] M. Urban, J. Noga, S.J. Cole, R.J. Bartlett, J. Chem. Phys. 83 (1985) 4041.
[52] K. Raghavachari, G.W. Trucks, J.A. Pople, M. Head-Gordon, Chem. Phys. Lett. 157 (1989) 479.
[53] S.F. Boys, F. Bernard, Mol. Phys. 19 (1970) 553.
[54] M. Gutowski, G. Chalasiñski, J. Chem. Phys. 98 (1993) 5540.
[55] B.D. Wladkowski, W.D. Allen, J.I. Brauman, J. Phys. Chem. 98 (1994) 13532.
[56] H. Wang, L. Zhu, W.L. Hase, J. Phys. Chem. 98 (1994) 1608.
[57] B.D. Wladkowski, A.L.L. East, J.E. Mihalick, W.D. Allen, J.I. Brauman, J. Chem. Phys. 100 (1994) 2058.

[58] J.L. Duncan, J. Mol. Spectrosc. 60 (1976) 225.
[59] J.L. Duncan, M.M. Law, J. Mol. Spectrosc. 140 (1990) 13.
[60] Data are taken from NIST online database, website: http://webbook.nist.gov.
[61] J.W. Larson, T.B. McMahon, J. Am. Chem. Soc. 105 (1983) 2944.
[62] Y. Yang, H.V. Linnert, J.M. Riveros, K.R. Williams, J.R. Eyler, J. Phys. Chem. A 101 (1997) 237.
[63] M.D. Harmony, V.W. Laurie, R.L. Kuczkowski, R.H. Schwendeman, D.A. Ramsay, F.J. Lovas, W.J. Lafferty, A.G. Maki, J. Phys. Chem. Ref. Data 8 (1979) 619.